50

SATELLITE & MESOMETEOROLOGY
RESEARCH PROJECT

Department of the Geophysical Sciences
The University of Chicago

EARLY STAGE OF TORNADO DEVELOPMENT AS REVEALED BY SATELLITE PHOTOGRAPHS

by

Tetsuya Fujita

(Chapter IV of a Comprehensive Study of the Palm Sunday Tornadoes, 1965)

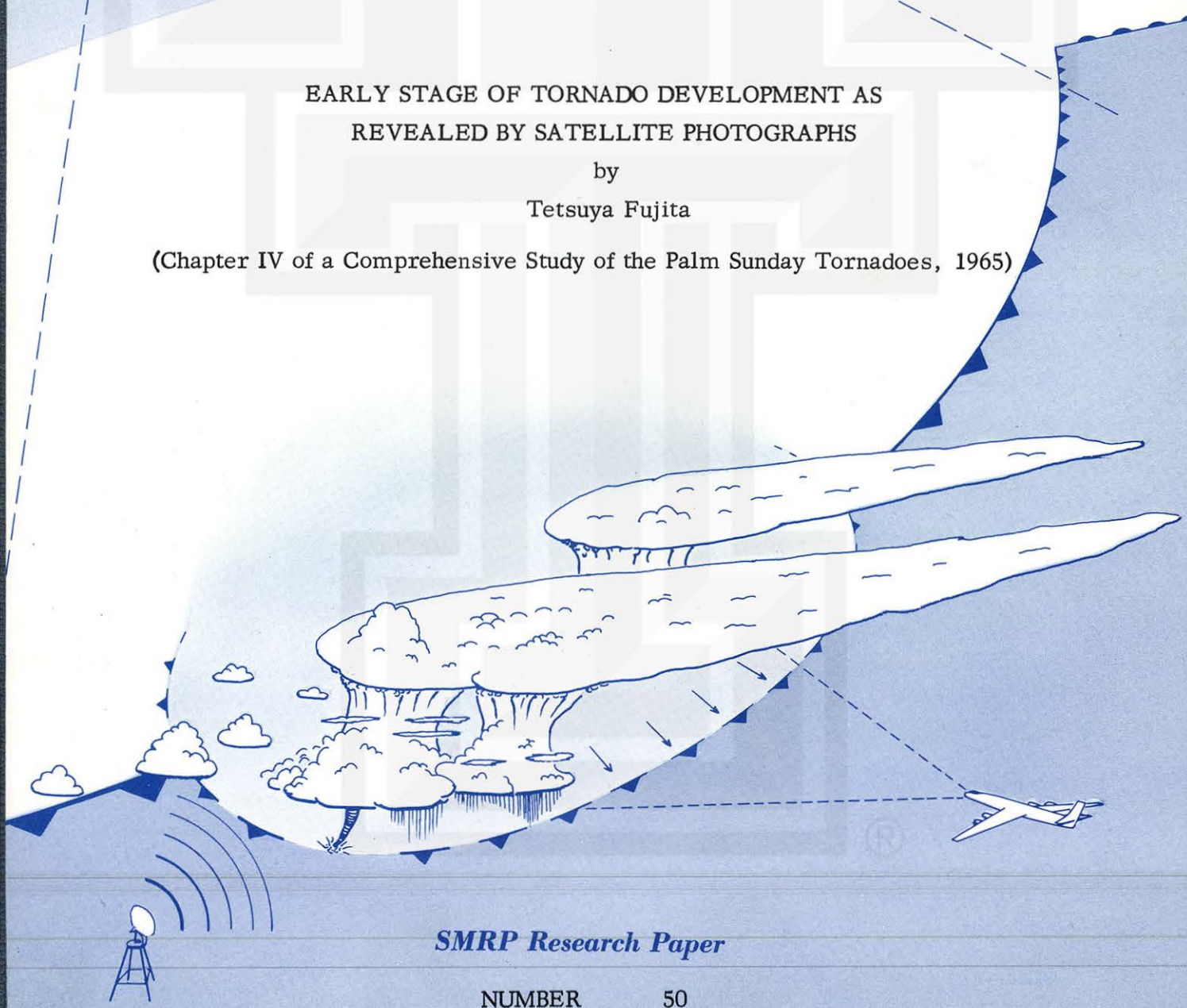

SMRP Research Paper

NUMBER 50

January 1966

MESOMETEOROLOGY PROJECT --- RESEARCH PAPERS

1.* Report on the Chicago Tornado of March 4, 1961 - Rodger A. Brown and Tetsuya Fujita

2.* Index to the NSSP Surface Network - Tetsuya Fujita

3.* Outline of a Technique for Precise Rectification of Satellite Cloud Photographs - Tetsuya Fujita

4.* Horizontal Structure of Mountain Winds - Henry A. Brown

5.* An Investigation of Developmental Processes of the Wake Depression Through Excess Pressure Analysis of Nocturnal Showers - Joseph L. Goldman

6.* Precipitation in the 1960 Flagstaff Mesometeorological Network - Kenneth A. Styber

7.** On a Method of Single- and Dual-Image Photogrammetry of Panoramic Aerial Photographs - Tetsuya Fujita

8. A Review of Researches on Analytical Mesometeorology - Tetsuya Fujita

9. Meteorological Interpretations of Convective Nephsystems Appearing in TIROS Cloud Photographs - Tetsuya Fujita, Toshimitsu Ushijima, William A. Hass, and George T. Dellert, Jr.

10. Study of the Development of Prefrontal Squall-Systems Using NSSP Network Data - Joseph L. Goldman

11. Analysis of Selected Aircraft Data from NSSP Operation, 1962 - Tetsuya Fujita

12. Study of a Long Condensation Trail Photographed by TIROS I - Toshimitsu Ushijima

13. A Technique for Precise Analysis of Satellite Data; Volume I - Photogrammetry (Published as MSL Report No. 14) - Tetsuya Fujita

14. Investigation of a Summer Jet Stream Using TIROS and Aerological Data - Kozo Ninomiya

15. Outline of a Theory and Examples for Precise Analysis of Satellite Radiation Data - Tetsuya Fujita

16. Preliminary Result of Analysis of the Cumulonimbus Cloud of April 21, 1961 - Tetsuya Fujita and James Arnold

17. A Technique for Precise Analysis of Satellite Photographs - Tetsuya Fujita

18. Evaluation of Limb Darkening from TIROS III Radiation Data - S.H.H. Larsen, Tetsuya Fujita, and W.L. Fletcher

19. Synoptic Interpretation of TIROS III Measurements of Infrared Radiation - Finn Pedersen and Tetsuya Fujita

20. TIROS III Measurements of Terrestrial Radiation and Reflected and Scattered Solar Radiation - S.H.H. Larsen, Tetsuya Fujita, and W.L. Fletcher

21. On the Low-level Structure of a Squall Line - Henry A. Brown

22. Thunderstorms and the Low-level Jet - William D. Bonner

23. The Mesoanalysis of an Organized Convective System - Henry A. Brown

24. Preliminary Radar and Photogrammetric Study of the Illinois Tornadoes of April 17 and 22, 1963 - Joseph L. Goldman and Tetsuya Fujita

25. Use of TIROS Pictures for Studies of the Internal Structure of Tropical Storms - Tetsuya Fujita with Rectified Pictures from TIROS I Orbit 125, R/O 128 - Toshimitsu Ushijima

26. An Experiment in the Determination of Geostrophic and Isallobaric Winds from NSSP Pressure Data - William Bonner

27. Proposed Mechanism of Hook Echo Formation - Tetsuya Fujita with a Preliminary Mesosynoptic Analysis of Tornado Cyclone Case of May 26, 1963 - Tetsuya Fujita and Robbi Stuhmer

28. The Decaying Stage of Hurricane Anna of July 1961 as Portrayed by TIROS Cloud Photographs and Infrared Radiation from the Top of the Storm - Tetsuya Fujita and James Arnold

29. A Technique for Precise Analysis of Satellite Data, Volume II - Radiation Analysis, Section 6. Fixed-Position Scanning - Tetsuya Fujita

30. Evaluation of Errors in the Graphical Rectification of Satellite Photographs - Tetsuya Fujita

31. Tables of Scan Nadir and Horizontal Angles - William D. Bonner

32. A Simplified Grid Technique for Determining Scan Lines Generated by the TIROS Scanning Radiometer - James E. Arnold

33. A Study of Cumulus Clouds over the Flagstaff Research Network with the Use of U-2 Photographs - Dorothy L. Bradbury and Tetsuya Fujita

34. The Scanning Printer and Its Application to Detailed Analysis of Satellite Radiation Data - Tetsuya Fujita

35. Synoptic Study of Cold Air Outbreak over the Mediterranean using Satellite Photographs and Radiation Data - Aasmund Rabbe and Tetsuya Fujita

36. Accurate Calibration of Doppler Winds for their use in the Computation of Mesoscale Wind Fields - Tetsuya Fujita

37. Proposed Operation of Intrumented Aircraft for Research on Moisture Fronts and Wake Depressions - Tetsuya Fujita and Dorothy L. Bradbury

38. Statistical and Kinematical Properties of the Low-level Jet Stream - William D. Bonner

39. The Illinois Tornadoes of 17 and 22 April 1963 - Joseph L. Goldman

40. Resolution of the Nimbus High Resolution Infrared Radiometer - Tetsuya Fujita and William R. Bandeen

41. On the Determination of the Exchange Coefficients in Convective Clouds - Rodger A. Brown

* Out of Print
** To be published

(Continued on back cover)

SATELLITE AND MESOMETEOROLOGY RESEARCH PROJECT
Department of the Geophysical Sciences
The University of Chicago

EARLY STAGE OF TORNADO DEVELOPMENT AS REVEALED BY SATELLITE PHOTOGRAPHS

by
Tetsuya Fujita

(Chapter IV of a Comprehensive Study of the Palm Sunday Tornadoes, 1965)

SMRP Research Paper #50
January 1966

The research reported in this paper has been supported by the U. S. Weather Bureau under grant Cwb WBG-41 and partially under grant Cwb WBG-34.

EARLY STAGE OF TORNADO DEVELOPMENT AS REVEALED BY SATELLITE PHOTOGRAPHS[1]

Tetsuya Fujita

Department of the Geophysical Sciences
The University of Chicago
Chicago, Illinois

ABSTRACT

About 20 min. after the first of a series of Palm Sunday tornadoes of April 11, 1965 formed in extreme eastern Iowa, TIROS IX, in northbound semi-polar Orbit No. 960, took pictures of the midwestern United States. Though the area of the tornado formation was too far from the exposure subpoint to be examined in detail, a vast region of southwesterly flow behind the cold front extending from Iowa to Arkansas was photographed with relatively small nadir angles of view. Of great interest was a faint, cirrus-like streak inside a large clear area behind the front, which, it was concluded, was a dust storm limiting visibility to less than two miles in some areas. Thermodynamical structure of the dry cold air in which the dust storm was embedded will be discussed in detail in connection with its role in giving rise to the development of the Palm Sunday tornadoes.

1. SYNOPTIC SITUATION AT 1200 CST, APRIL 11, 1965

The synoptic situation during a 24-hr. period, 0600 CST, April 11 through 0600 CST, April 12, 1965, was discussed in Chapter 3 by Van Thullenar. Only one TIROS photographic pass is available for this period. Two of the best pictures covering the areas were exposed at 12h 41.3m and 12h 42.3m CST about 20 min. after the formation of the first tornado. A detailed analysis of synoptic charts for 1200 CST was made in an attempt to learn the structure of the atmosphere over the region of the tornado formation.

A deep continental cyclone with a central pressure of 985 mb. was moving east-northeastward over Iowa. A weak warm front extending eastward from its center was interrupted by a dissipating mesohigh designated as "E" in figure 1. To the south of this warm front, southerly winds of 15 to 25 kt. were transporting moist

[1]The research reported in this paper has been supported by the U. S. Weather Bureau under grant Cwb WBG-41 and partially under grant Cwb WBG-34.

warm air with T_d above 60F toward the front. The area of this moist warm air is designated "A".

Behind this air mass "A", a rather cold but extremely dry air mass "B" was pushing eastward, thus forming a sharp dry cold front extending from the cyclone center to Arkansas. This air mass "B" was followed by relatively moist cold air "D" which was pushing southeast from Wyoming. As the air mass "B" moved over the Rockies in Colorado, it became much drier than the air mass "D". Air mass "C" is of maritime polar origin with easterly winds up to about 20 kt.

An isotherm chart for 1200 CST covering the area of the surface isobar chart is shown in figure 2. The warmest spot in the warm sector "A" is located to the south of St. Louis, Missouri, with a temperature of over 85F. A cold spot near Louisville, Kentucky and another near Dubuque, Iowa are associated with local thunderstorm activities within the warm sector.

Within air mass "B", the air temperature gradually decreases westward from 80F near the dry cold front to about 45F along the foothills of the Rockies. Air mass "D" is colder than "B", due to the fact that "D" slipped out from the northwest without moving over the high Rocky Mountains.

The horizontal temperature gradient within air mass "C" is the greatest of all the air masses surrounding the continental cyclone centered over Iowa. Because of the surface temperature of Lake Michigan, there existed a marked cold temperature ridge over the lake, thus creating 10 to 20F temperature drops between stations located on the east and west sides of the lake.

The most significant contrasts between the air masses A, B, and D are seen in an isodrosotherm chart of figure 3. The dew-point temperature within the warm sector is fairly uniform, varying only between 60 and 70F. A significant drop in the rear of the cold front results in 20F near Kansas City, Missouri and there is a further drop to only 6F in the northwest corner of New Mexico. Since the dew-point temperatures from the mountain stations are as high as 20 to 22F, we may suspect that the extreme dryness east of the Rockies was caused by the mesoscale blocking action of the Rockies. The dew-point temperature inside the air mass "D" is at least 10F higher than that of "B". A line with short spikes dividing these two air masses designates a front, the passage of which produces a drop in temperature and a simultaneous increase in dew-point temperature. Such a front may be called the "moist cold front". On the other hand, a line dividing air masses "A" and "B" is a

cold front in nature, but it is accompanied by a marked drop in dew-point temperature. To distinguish this cold front from the former, it is called the "dry cold front."

For the purpose of determining those areas where visibility is obstructed due to smoke (K), fog (F), haze (H), dust (D), and precipitation near the ground, horizontal visibilities were plotted and contoured as in figure 4. Either fog or fog mixed with drizzle (LF) is seen practically everywhere inside the moist cold air mass "C". In some spots visibilities of one mile with fog are reported. Inversion-trapped haze and smoke are reported from a half a dozen stations on the downwind side of the Detroit area. A relatively low visibility reported inside the mesohigh "E" is mostly due to rain fog caused by early morning shower activity.

The warm sector "A" is free from fog and the visibility is more than 7 miles practically everywhere. With the exception of the northernmost area, visibility inside the warm sector increases near the dry cold front. To the west of the front visibility increases from 10 to 15 miles. This might have been much better had further distant ground objects been available to observers. It should be noted that a zone with over 15-mile visibility extends about 150 miles behind the dry cold front. To the west of this zone there is an island of low visibility, down to 2 miles, caused mainly by dust (D) and blowing dust (BD), according to the station reports. Since this area of dust is extremely large, it is seen in satellite pictures and will be discussed later in this chapter. Significant increases in visibility to the west of this dust area may simply be due to the fact that observers can use mountains as ground objects. Nevertheless, such excellent visibility strongly suggests the existence of a foehn phenomenon on the leeward side of the Rocky Mountains.

2. SATELLITE PHOTOGRAPHS AND SIGNIFICANT CLOUD FEATURES

A series of photographs was taken by TIROS IX in Orbit 960 as it passed over the Rockies toward the north-northwest. Of these pictures, Frames 9 and 10, exposed at 12h 42.3m and 12h 41.3m CST, respectively, show the best coverage of the areas of interest. They were therefore gridded as precisely as possible with the use of the graphical method developed by Fujita (1963). Figures 5 and 6 show these photographs with state boundaries superimposed.

A significant feature appearing in figure 5 is a large tongue of clear area extending from New Mexico to Missouri. Faint streaks stretching from the Oklahoma Panhandle to southern Kansas are located in the area of low visibility caused by

blowing dust (see figure 4). This is the first time that a large area of dust storms appearing on a satellite picture over the midwestern United States has been reported, thus raising some questions regarding the reflectance of dust clouds. Satellite pictures often show dust clouds extending from desert regions to nearby ocean surfaces. In such cases, dust clouds are easily distinguished against the dark ocean background. Over the midwestern United States, however, relatively large ground reflectance makes it very difficult to detect dust clouds unless they are very dense and extend to high altitudes. Based upon the isentropic analysis which appears in the following section, the top of the dust clouds under discussion was estimated to be about 9,000 ft. above the ground.

Frame 10, exposed at 12h 41.3m CST, reveals a mesoscale eddy of dust clouds over the Kansas-Oklahoma border. Scattered small clouds spreading from Colorado to central Kansas are cumuli with their bases at about 6,000 ft. above the ground. Two areas of jet stream cirrus are located over central and eastern Texas. Along their northern boundaries thin shadows are visible as irregular wavy lines.

These two frames, gridded with one-degree geographic grids, were used in constructing a nephanalysis chart (see figure 7) on which radar echoes are also entered. These echoes were obtained from WSR-57 radar photographs taken at the Minneapolis, Chicago, and Detroit Weather Bureau stations. When this nephanalysis chart is studied together with isobar, isotherm, isodrosotherm, and visibility charts, it becomes evident that a group of scattered echoes is located along a zone north of the warm front extending in an east-west direction through the center of the major continental cyclone. The satellite photographs show that anvil clouds extend east-northeastward from many of these cells. Only a few remaining echoes are seen inside the mesohigh area to the south of Lake Erie. This system is now in its dissipating stage.

Due to about a 45-min. time difference between the 1200 CST chart and the satellite photographs, the southwestern edge of line echoes in northeastern Iowa and the leading edge of the dry cold front do not coincide precisely. The echoes are located about 40 miles to the east of the front, suggesting that they were very close to the position of the dry cold front 45 min. later. If we follow the line echoes beyond the southeastern end, we see that clouds without echoes are located along the dry cold front in Iowa. In Missouri, however, the cloud line extends in a northeast-southwest direction inside the dry cold air mass "B".

For further interpretation of this cloud line and others, a detailed neph-

analysis (figure 8) chart was made by plotting surface reports at 1200 CST. Cloud covers N_h and $(N - N_h)$ were entered inside each station circle as painted and hatched areas, respectively. Cloud symbols are conventional ones except T, that refers to towering, and the double subscripts C_{ii} , C_{ss} , that represent thick cirrus and cirrostratus clouds, respectively. A polar jet stream extends from southwest to northeast. A large area of jet-stream cirrus is seen in Texas to the south of the jet stream. Another area of cirrus extending from Louisiana eastward seems to be associated with shower activity along the southern end of the dry cold front.

A stippled area in the northern part of the nephanalysis chart represents low stratus overcast mixed with fog. A band of stratocumulus cover extending from Louisiana to Ohio corresponds to the tongue of moist air transported from the gulf by a strong low-level jet with up to 50 kt. winds. From early morning of April 11, several mesoscale convective activities took place, thus leaving areas of low stratus and stratocumulus over northwestern Louisiana, southwestern Tennessee, and southern Ohio.

The stations within the area of faint cirrus-like clouds in the satellite pictures (figures 5 and 6) reported dust. Not a single station within the vicinity of the dust area reported cirrus or cirrostratus, thus eliminating the possibility that the faint clouds consist partially of high clouds. It should be noted that the northwestern tip of the dust area is bent along the moist cold front as shown in the figure.

A cloud line extending southwest to northeast in central Missouri was reported as towering altocumuli from Springfield, Missouri. Their bases are 8,000 or nearly 9,000 ft. above the ground, suggesting that they formed near the top of the unstable dry air behind the dry cold front. Due to the extremely low mixing ratio in this air mass, most of the stations reported clear. If we somehow increase the surface dew-point temperature by 10C, it is quite feasible to create high-base cumuli or altocumulus castellanas near the top of the stable layer which characterizes this air mass. From this consideration and the fact that the orientation of the cloud line is identical to the direction of the mean winds below 9,000 ft., we may assume that a number of artificial lakes and large areas of forest in the Ozark Mountains gave rise to the increment of low-level moisture required to form high-level convective clouds.

3. STRUCTURE OF A DRY COLD AIR MASS

Studies of satellite photographs, including nephsystems that produce severe

storms, are relatively few in number. Of these, papers by Whitney and Fritz (1961), Fujita et al. (1963), and Whitney (1963) revealed that those nephsystems in their stages of severe-storm formations are characterized by their massive appearance, mostly elliptic but sometimes square-looking. This is due to the fact that anvil clouds produced by each of the cumulonimbus clouds over considerable areas, thus forming a large oval-shaped boundary when viewed from satellite altitudes. Satellite photographs taken approximately at the onset time of the Palm Sunday tornadoes (figure 5) revealed the existence of a large tongue of a clear area behind a line of expected tornado formations. The nephsystems associated with severe storms were not as extensive as reported in the above-mentioned papers, with the exception of a large cloud area from which no tornadoes were reported. The main reason is that the pictures were taken around local noon when nephsystems are still in their early stages of development. Thus the tongue of clear area should be investigated in detail as a cause of intense convective activity which gave rise to the development of an unusual number of tornadoes.

Soundings from Columbia (CBI), Missouri made at 12 and 18 CST, 3 and 9 hours after the passage of the dry cold front, appear in figure 9. A common but important characteristic in these soundings is the deep layer of dry-adiabatic lapse rate topped by a rather stable layer in which a 10C rise in the potential temperature was observed. In other words, the entropy below 780 mb. at 1200 CST was practically constant and expressed by 301K. Six hours later the top of the 297K isentropic layer was at 750 mb., indicating a slight lifting.

When the pressures at the top of the isentropic layer behind the dry cold front were plotted in figure 10, a dome of isentropic air mass reaching 580 mb. over New Mexico was found. The contour lines of this dome-top pressure and the mean wind velocities inside the dome reveal that the air originated over the Southwest desert region and was drawn into the southwestern sector of a well-developed continental cyclone centered in southern Wisconsin. It is important to realize that the entropy is constant along the vertical anywhere within the dome. In horizontal directions, however, the entropy varies between the highest, 308K at El Paso, and the lowest, 288K at North Platte. Dashed lines in figure 10 are the isentropes of the surface potential temperatures drawn for every 5K.

East of the dry cold front, the isentropic surfaces intersecting the surface along these isentropes slope up toward the north and northeast. Inside the dome behind the dry cold front, however, the isentropic surfaces are the vertical walls

standing above the isentropes. These walls are no longer vertical beyond the dome top. The isentropic flow inside the dome should, therefore, be limited within these vertical walls on which air may freely move up and down, accomplishing large-scale vertical mixing as it travels eastward. In order to visualize such a motion, a vertical cross-section of potential temperatures and winds was made along the 297K isentrope inside the dome and its extension outside the dome. This cross-section extends from Tucson to Buffalo, crossing over the Rocky Mountains (figure 11). Since this vertical cross-section is made to include a vertical wall of 297K isentropic surface inside the dome of dry cold air mass, we may assume that the air mass was unstable and almost vertically mixed as it traveled from the southwest arid region to the Midwest. As expected, the elevation of the dome top reached its highest over the Rockies, sloping down toward the east. The dust cloud seen in the satellite pictures may have extended to the top of the dome, some 9,000 ft. above the ground. This is probably part of the reason why such views of dust clouds appeared in the pictures.

This dome of isentropic air is topped by a significant stable layer of about a 3,000-ft. thickness. Within this layer, wind speed increased to about 100 kt. while the leading edge of the dome or the dry cold front was moving at about 50 kt. This relative motion of 50 kt. eastward results in a significant downslope motion of mid-tropospheric westerlies above the dome.

Cold Advection Near the Dome Top. Due to the dry-adiabatic lapse rate inside the dome west of the dry cold front and the rather stable lapse rate inside the warm sector ahead of the front, the temperature difference between the warm moist and the cold dry air increases more or less in proportion to the height above the ground. At the dome top at about 700 mb., the temperature was about 5C colder than the warm moist air east of the dry cold front. In terms of virtual temperature the dome was about 6C colder.

When the cold air near the top of the dome is advected eastward at the rate of about 50 kt., it runs over the warm moist air, thus creating a super-adiabatic lapse rate within the warm air below the dome-top level. The warm moist air then overturns quickly along the leading edge of the dome top, thus initiating vigorous convection along the line. The location of the surface dry cold front is not necessarily directly beneath the leading edge of the dome, the latter usually being seen 10 to 50 miles to the east of the former.

4. CONCLUSIONS

Through studies of satellite photographs taken within one hour after the formation of the first tornado on April 11, 1965, it was found that a tongue of clear area including large dust storms was closely related to the development of the violent convection giving rise to the formation of an unusually large number of tornadoes on Palm Sunday. First of all, the visual boundary of a clear-air tongue permits us to determine the leading edge of the dry cold air. Secondly, the dust storm clouds clearly visible against the ground surface suggest the extreme thickness of the dust, that is, the height of the isentropic dome.

The concept of cold advection as well as warm advection in relation to severe-storm development has been discussed by Fulks (1951), Winston (1953), Suggs and Foster (1954), Whitney and Miller (1956), and others. The situations that they studied involved rather moderate horizontal transport of cold air aloft and/or warm air below, resulting in a significant change in stability. In this current case, however, cold advection took place near the top of the dome of dry cold air as it plowed rapidly eastward, with a dramatic overturning taking place along the leading edge of the plowing air.

It is recommended that more cases of severe-storm development be studied with the use of satellite pictures taken around local noon so as to investigate the relatively early stages of storm development in which the areas of anvil shield are still rather small.

REFERENCES

Fujita, T., 1963: A Technique for Precise Analysis for Satellite Data; Volume I - Photogrammetry, MSL Report No. 14, U. S. Weather Bureau.

_____, T. Ushijima, W.A. Hass, G.T. Dellert, Jr., 1963: Meteorological Interpretation of Convective Nephsystems Appearing in TIROS Cloud Photographs. Proceedings of the First International Symposium on Rocket and Satellite Meteorology, Washington, D.C., 357-387.

Fulks, J.R., 1951: The Instability Line, Compendium of Meteorology, Amer. Meteor. Soc., 647-652.

Sugg, A.L., and D.S. Foster, 1954: Oklahoma Tornadoes, May 1, 1954. Mon. Wea. Rev., 82, 131-140.

Whitney, F.L. Jr., and J.E. Miller, 1956: Destabilization by Differential Advection in the Tornado Situation of 8 June 1953. Bull. Amer. Meteor. Soc. 37, 224-229.

_____, and S. Fritz, 1961: A Tornado-Producing Cloud Pattern seen from TIROS I. Bull. Amer. Meteor. Soc., 42, 603-614.

_____, 1963: Severe Storm Clouds as seen from TIROS. J. Appl. Meteor., 2, 501-507.

Winston, J.S., 1953: The Weather and Circulation of May 1953 -- One of the Worst Tornado Months on Record. Mon. Wea. Rev., 81, 135-140.

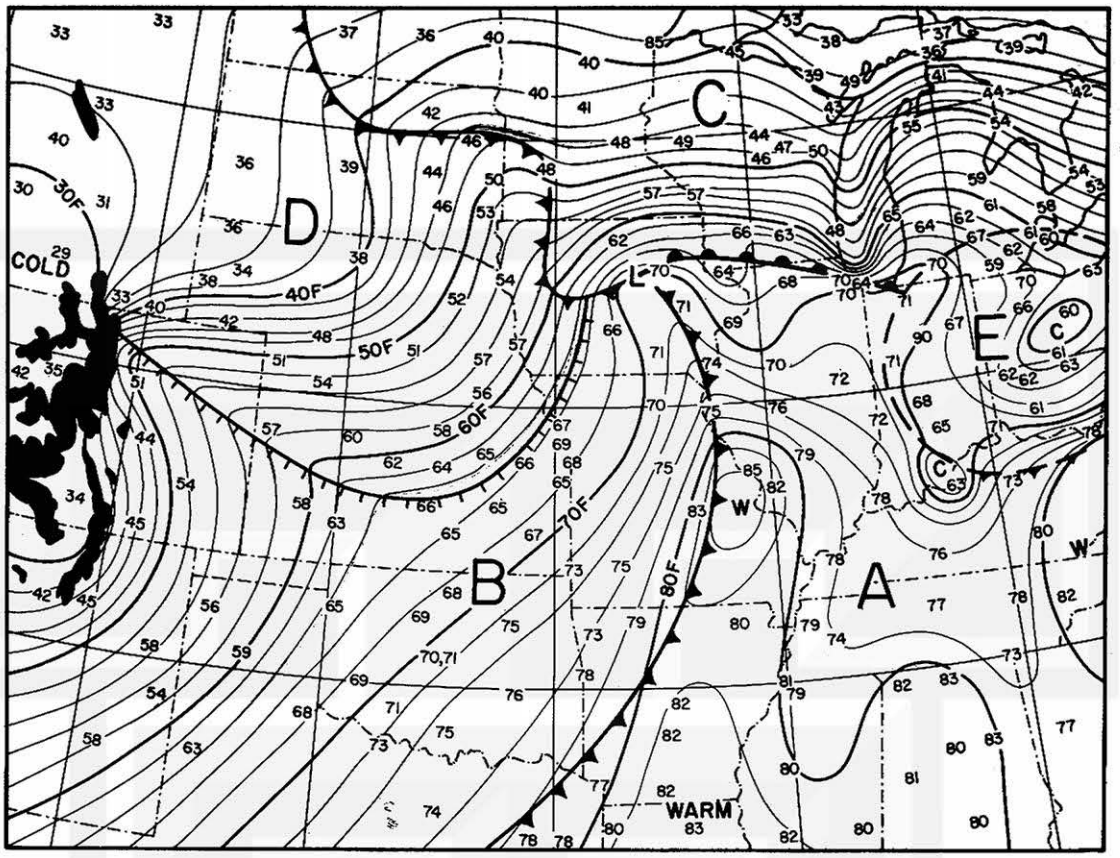

FIGURE 1. Surface winds and isobars at 1200 CST, April 11, 1965. A long wind barb and a flag were drawn to represent 5 kt. and 25 kt., respectively, in order to emphasize the intensity of surface winds. Air masses involved are: A, moist warm air; B, dry cold air; C, moist colder air; D, moist cold air; and E, outflow from a dissipating mesohigh.

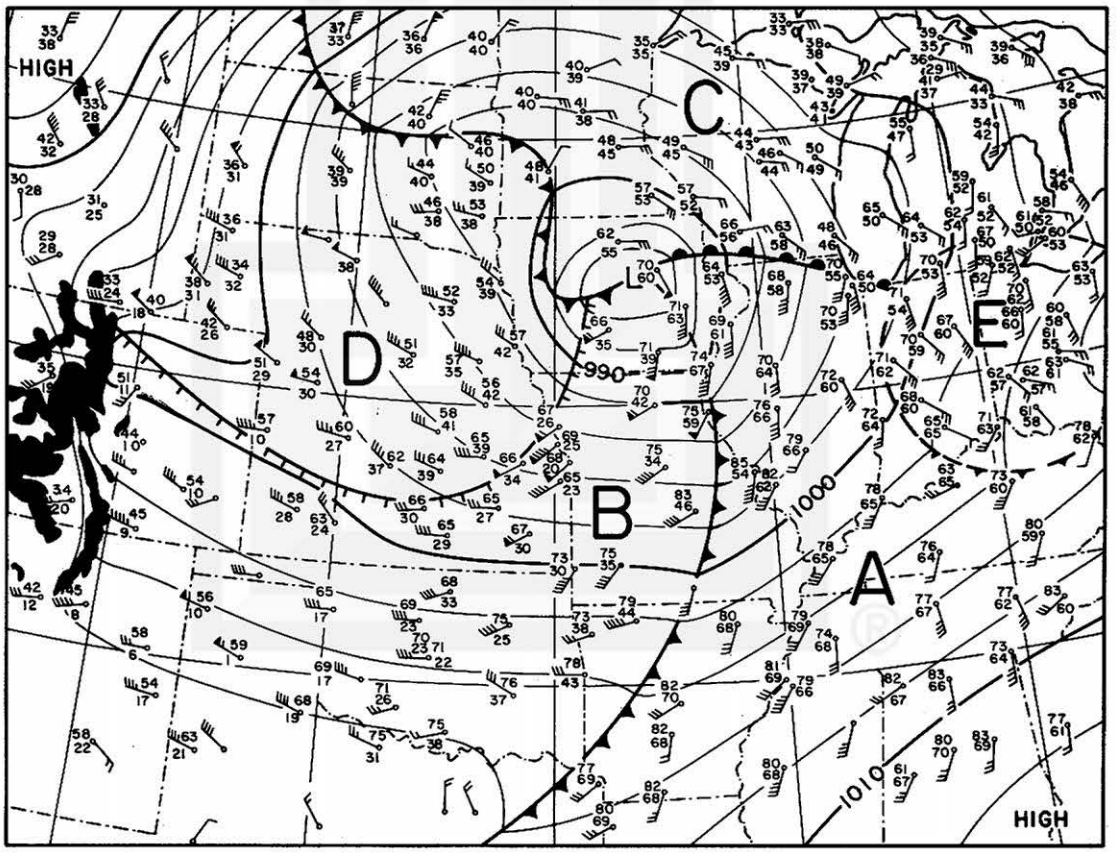

FIGURE 2. Isotherms at 1200 CST, April 11, 1965 contoured for every 2F.

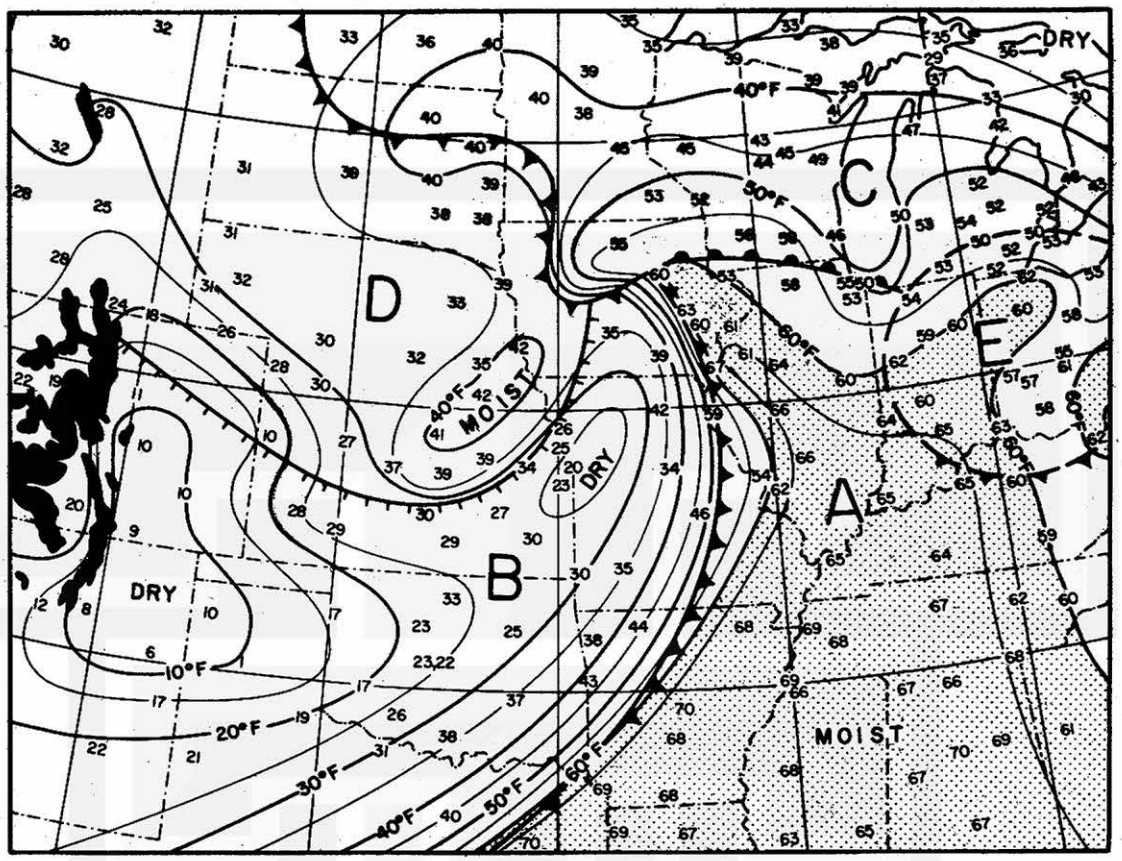

FIGURE 3. Isodrosotherms at 1200 CST, April 11, 1965 contoured for every 2F. Areas of air temperature above 60F are stippled.

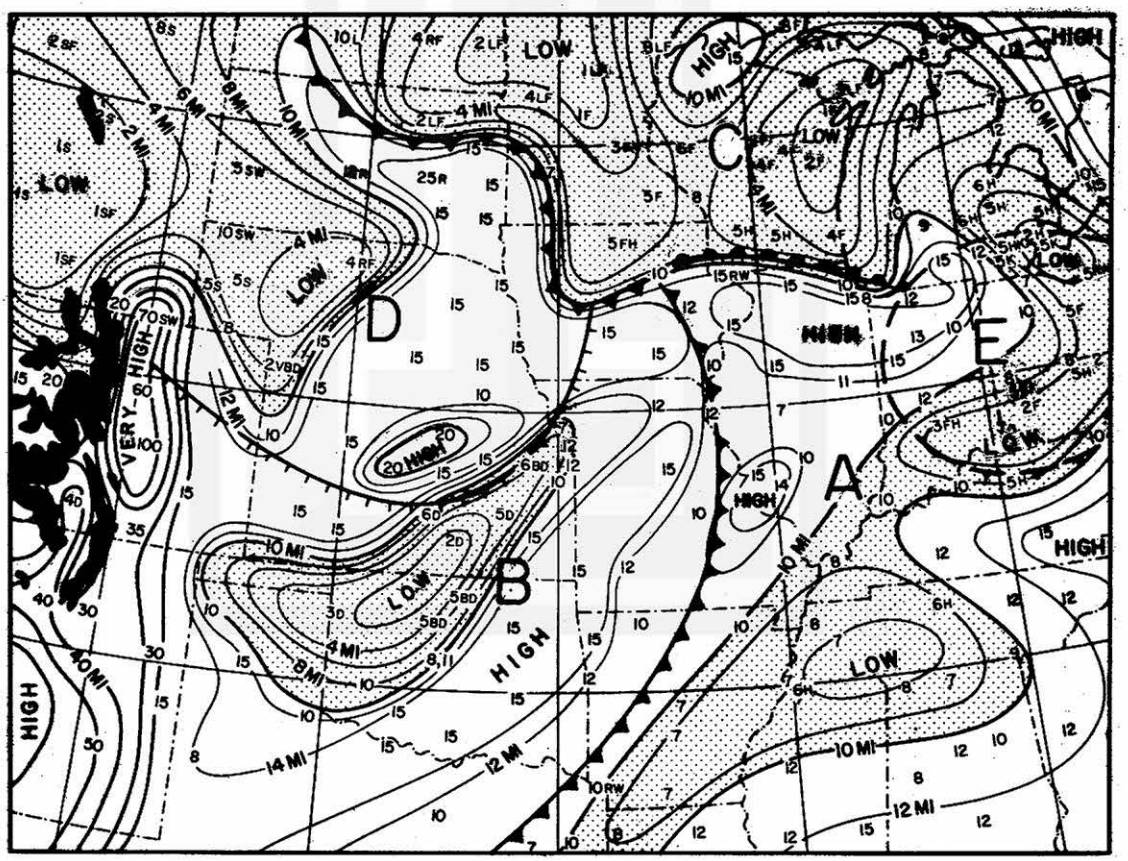

FIGURE 4. Visibility chart for 1200 CST, April 11, 1965. Contoured for every 2 miles with thin contours and for every 10 miles with heavy contour lines. Areas of visibility lower than 10 miles are stippled.

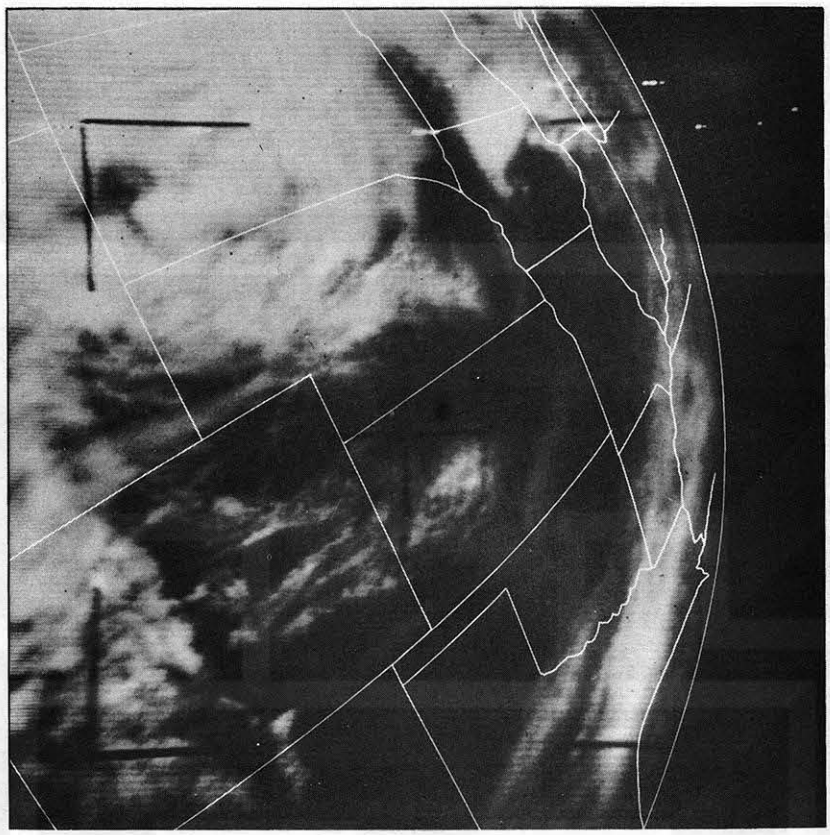

FIGURE 5. Satellite picture showing clear areas behind the dry cold front. TIROS IX, Orbit 960, Frame 9 exposed at 12h 42.3m CST, April 11, 1965. Photogrammetric data: H=801 km, ϕ^{TSP}= 42.4N, θ^{TSP}=112.7W, α^{PP} =116°, and τ = 35.6°.

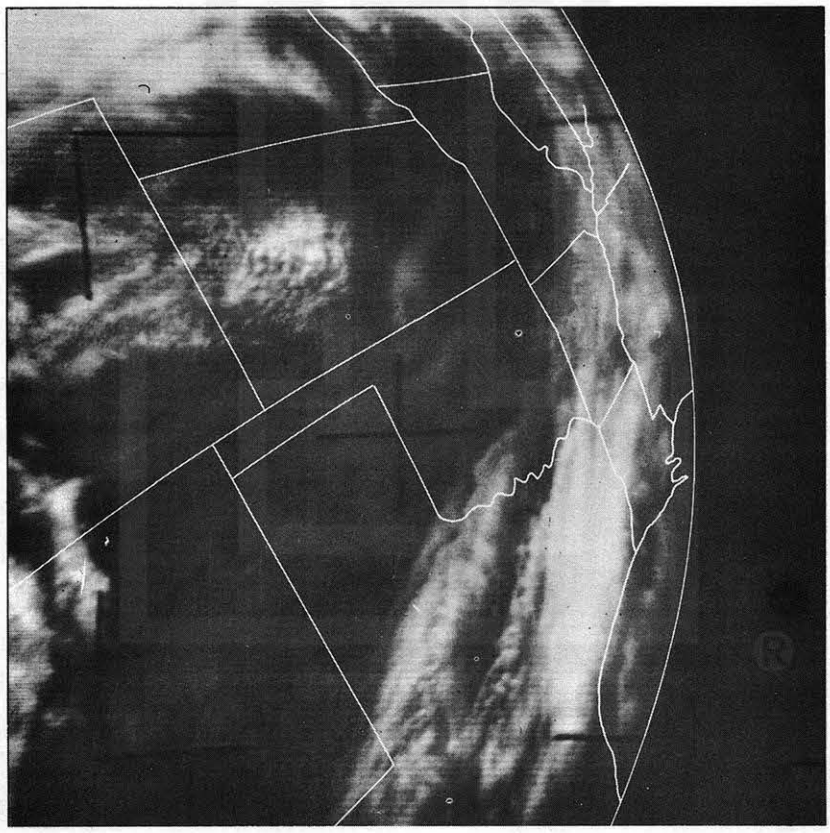

FIGURE 6. Satellite picture showing dust storm inside the clear area. TIROS IX, Orbit 960, Frame 10 exposed at 12h 41.3m CST, April 11, 1965. Photogrammetric data: H=778 km, ϕ^{TSP}= 38.4N, θ^{TSP}=113.7W, α^{PP}=116°, and τ = 38.0°

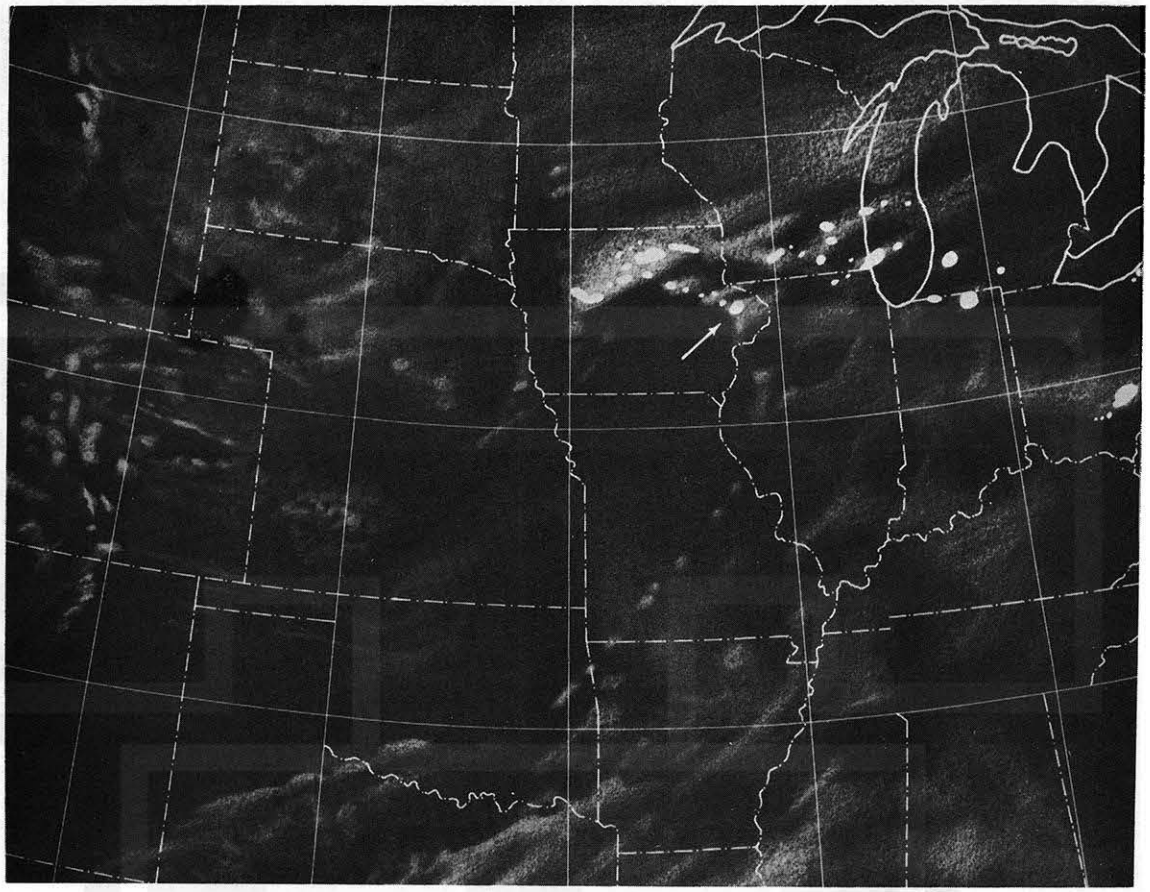

FIGURE 7. Nephanalysis covering midwestern United States at 1240-43 CST, April 11, 1965. The echo which produced the first tornado, about 20 min. earlier, is indicated by an arrow in Iowa. White spots are radar echoes at the time of satellite pictures used in making this nephanalysis.

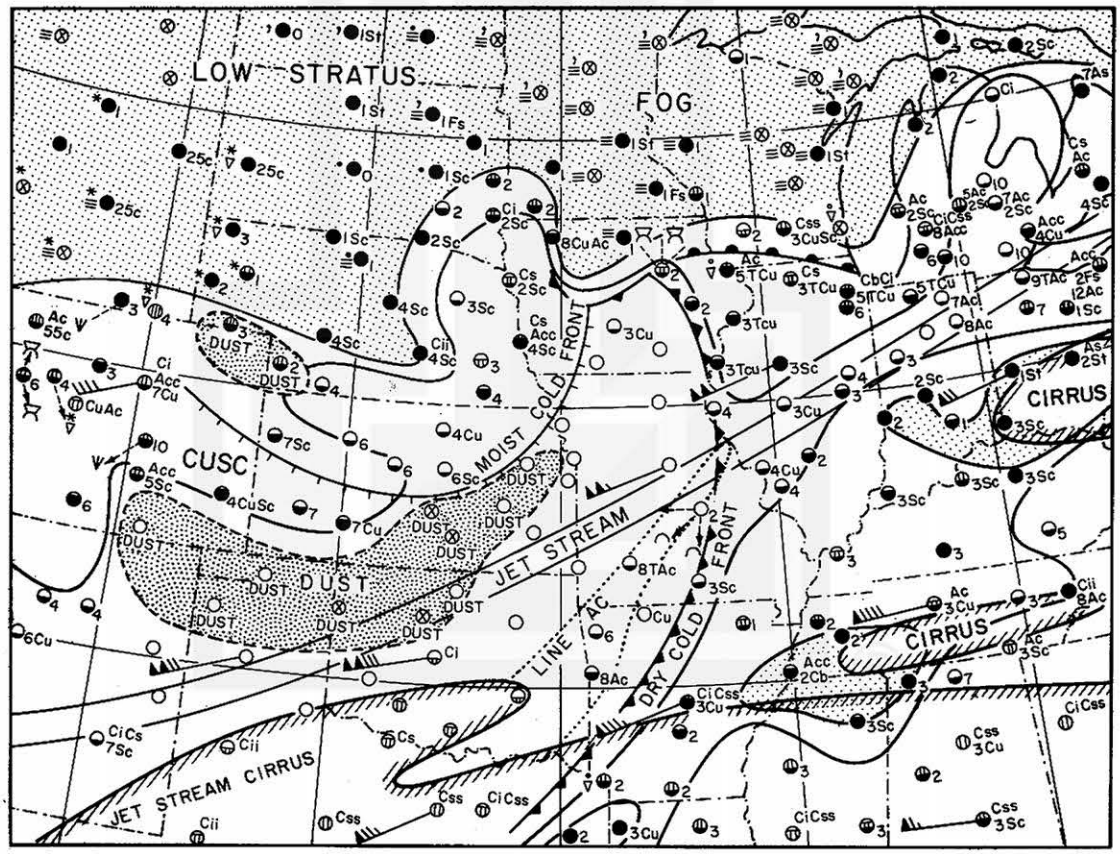

FIGURE 8. A cloud chart for 1200 CST, April 11, 1965 constructed on the basis of surface reports. The covers of low and other clouds are shown in each station circle by black and hatched areas, respectively. Numbers preceeding cloud types indicate the cloud base in 1000 ft. 300-mb. winds for 1200 CST are also entered with conventional symbols.

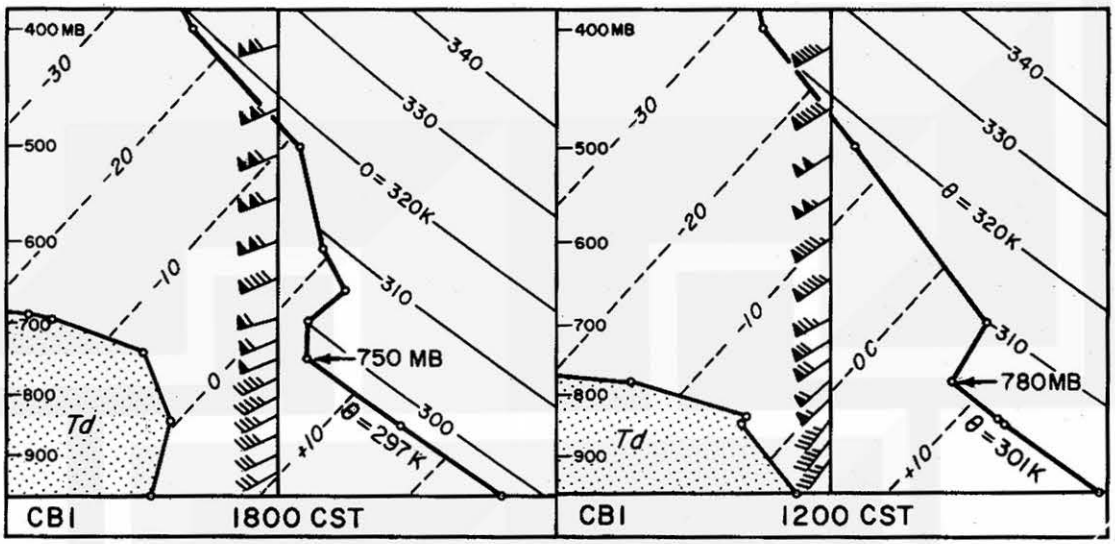

FIGURE 9. Soundings from Columbia, Missouri made at 1200 and 1800 CST, April 11, 1965. Note increase in height of the deep isontropic layer above the ground. Soundings were made inside the dry cold air mass in which the isentropic surfaces are curved vertical walls.

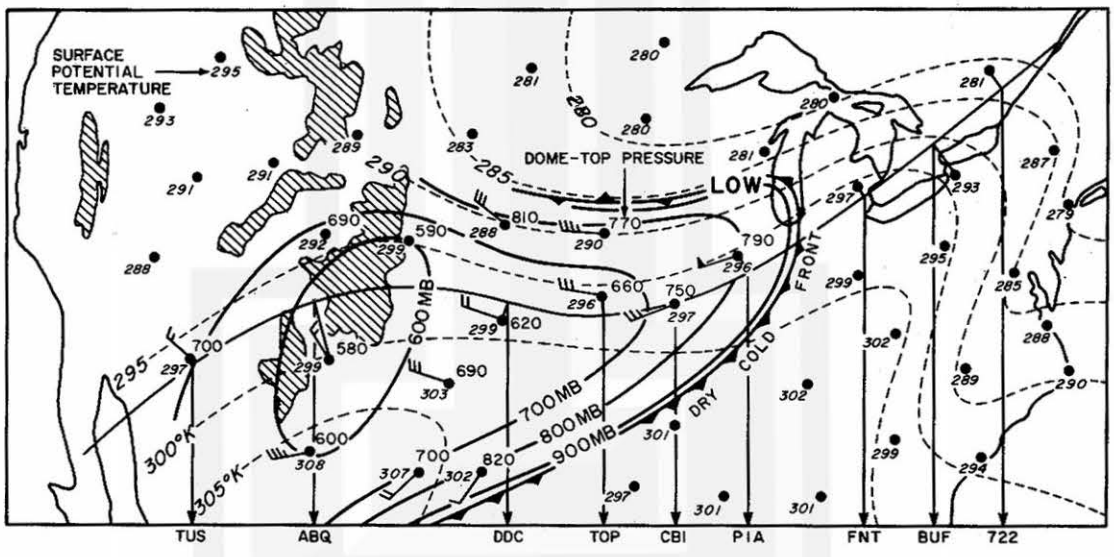

FIGURE 10. Topography of the top of the dry cold air mass at 1800 CST, April 11, 1965. The highest portion of the dome is seen over the Colorado Rockies. Winds represent the vector mean of wind velocities inside the dry cold air. The potential temperatures at the ground are entered by each station in K. A vertical cross-section in the next figure was made along a curved line extending from Tucson to near Buffalo.

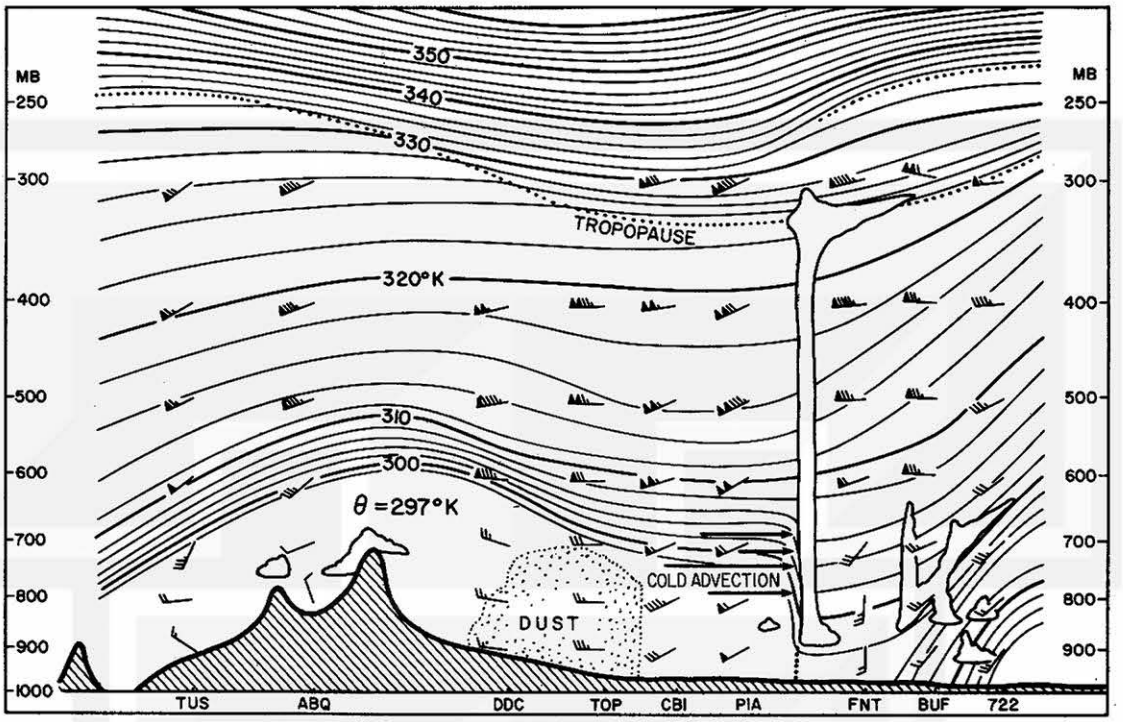

FIGURE 11. Vertical cross-section along 297K isentrope and its extension outside the dry cold air at 1800 CST, April 11, 1965. There was little temperature difference on either side of the dry cold front between Peoria and Flint. Due to a steep lapse rate to the west of the front, significant cold advection is seen near the 700-mb. surface located below a stable layer topping the isentropic flow from the west.

MESOMETEOROLOGY PROJECT ---- RESEARCH PAPERS

(Continued from front cover)

42. A Study of Factors Contributing to Dissipation of Energy in a Developing Cumulonimbus - Rodger A. Brown and Tetsuya Fujita

43. A Program for Computer Gridding of Satellite Photographs for Mesoscale Research - William D. Bonner

44. Comparison of Grassland Surface Temperatures Measured by TIROS VII and Airborne Radiometers under Clear Sky and Cirriform Cloud Conditions - Ronald M. Reap

45. Death Valley Temperature Analysis Utilizing Nimbus I Infrared Data and Ground-Based Measurements - Ronald M. Reap and Tetsuya Fujita

46. On the Thunderstorm - High Controversy - Rodger A. Brown

47. Application of Precise Fujita Method on Nimbus I Photo Gridding - Lt. Cmd. Ruben Nasta

48. A Proposed Method of Estimating Cloud-top Temperature, Cloud Cover, and Emissivity and whiteness of clouds from short- and Long-wave Radiation Data Obtained by TIROS Scanning Radiometers - T. Fujita and H. Grandoso

49. Aerial Survey of the Palm Sunday Tornadoes of April 11, 1965 - Tetsuya Fujita